

Benthic–Pelagic coupling over a zebra mussel reef in western Lake Erie

Josef Daniel Ackerman

Physical Ecology Laboratory, University of Northern British Columbia, Prince George, British Columbia, Canada V2N 4Z9

Mark R. Loewen¹

Civil and Environmental Engineering, University of Alberta, Edmonton, Alberta, Canada T6G 2G7

Paul F. Hamblin

National Water Research Institute, Burlington, Ontario, Canada L7R 4A6

Abstract

We conducted a field study including a series of cruises over an isolated offshore zebra mussel reef (7–11 m deep) in Western Lake Erie to examine the effect of zebra mussels (*Dreissena* spp.) on the water column. The horizontal currents over the reef were found to be primarily due to the hydraulic flow and surface gravitational seiches. The turbulence generated by these currents was found to be too weak to fully mix the water column. Although seasonal stratification was not observed, solar heating during the day and intrusions of cold central basin water caused stable stratification of the water column 60% of the time. Results from the seston analysis taken at five depths showed a statistically significant mussel-feeding signature in chlorophyll *a* and organic seston concentrations measured within 2 m above the reef. Estimates of clearance rates based on field data were consistent with rates measured in a flow chamber using water from the site, which indicated that zebra mussels could remove up to 40% of the total seston. The detection of a zebra mussel-induced concentration boundary layer is due to: (1) reduced vertical mixing as a result of semidiurnal periodic stratification, (2) refiltration of bottom water in zebra mussel populations, and (3) in situ clearance rates that are lower than those observed in the laboratory. Thus, offshore zebra mussel colonies may have less of an effect on the water column than had been previously estimated by simple stirred reactor models, and the role of zebra mussels in the clarification of Lake Erie should be investigated further.

There has been considerable interest as to whether aquatic ecosystems are controlled by limits to primary production by phytoplankton or by consumption by grazers (e.g., bottom up and top down controls, respectively; Fretwell 1987; Dame 1996). In the former, lack of nutrients is responsible for limits to phytoplankton growth, whereas in the latter, pelagic grazing of phytoplankton is the limiting factor. Benthic suspension feeders, such as bivalves, also contribute to the consumption of phytoplankton under certain conditions. This coupling of benthic and pelagic systems is a function of water depth, the physical processes that cause mixing in the water column, and the availability of phytoplankton to the benthos. The ability of suspension-feeding bivalves to control the algal biomass in the overlying water column has been investigated in the laboratory and through numerical modeling (Cloern 1991; Koseff et al. 1993; O’Riordan et al.

1995). The formation of concentration boundary layers has been observed over marine bivalves in tidal estuaries, and numerical models have confirmed that turbulent transport is the key physical process supplying phytoplankton to the bivalves (Fréchette et al. 1989).

Laboratory flume experiments have shown that the turbulent transport of phytoplankton to the suspension-feeding bivalves is determined by the dynamics of the momentum boundary layer (O’Riordan et al. 1995). Biological factors, such as variations in the quality and quantity of the food and the filtration rate, have a significant influence on the properties of the corresponding concentration boundary layer (Butman et al. 1994; Wildish and Kristmanson 1997). Although these studies have been conducted under unidirectional, largely tidally driven conditions, the situation in lakes is less well characterized because of the interaction of many forcing functions that control vertical mixing in the benthic boundary layer (Fischer et al. 1979), including (1) shear-produced turbulence at the bottom, (2) wind-driven surface waves, (3) surface gravitational seiches, (4) wind-driven horizontal circulation, (5) hydraulic flow, and (6) the earth’s rotation (Bedford and Abdelrhman 1987).

The introduction and rapid population growth of zebra mussels (*Dreissena* spp.) in the Laurentian Great Lakes in the 1980s (Hebert et al. 1991) provides an excellent opportunity to examine the issue of benthic–pelagic coupling in lakes. These introduced benthic suspension feeders have achieved ecologically dominant status in the benthos, unlike native sus-

¹ Corresponding author (mrloewen@civil.ualberta.ca).

Acknowledgments

The authors thank J. Bull, M. MaWhinney, R. Rowsell, and S. Smith of Environment Canada (CCIW) for deployment and operation of the field instruments; Daniel Levesque, Pierluigi Cozzi, and Randy Eaton (Crystal Charters) for assistance in the field and in the laboratory; and Dr. Dick Zimmerman, Dr. Myrna Jacobson, Dr. Peter Jackson, and Dr. Ann Zimmerman for valuable discussion.

The Great Lakes University Research Fund (Environment Canada and NSERC), the University of Toronto, and NSERC are gratefully acknowledged for providing funds to undertake this study.

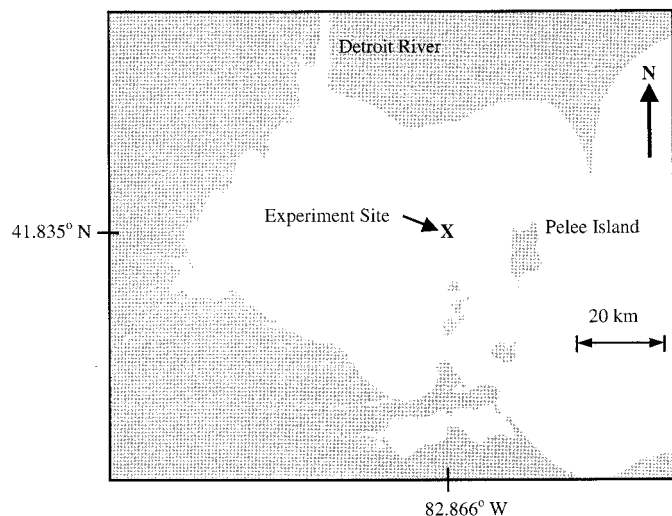


Fig. 1. The experimental site was ~ 1 km from North Harbor Island in western Lake Erie (X— 41.835°N , 82.866°W).

pension feeders, and have been implicated in the reduction of phytoplankton biomass and the clarification of water, particularly in Lake Erie (Nalepa and Schloesser 1993). This assertion is supported by observed mussel densities as high as 10^5 mussels m^{-2} , and when this is combined with their relatively high clearance rates, an extremely high areal clearance rate is predicted (e.g., MacIsaac et al. 1992; Nalepa and Schloesser 1993). This simple reactor model approach has led some researchers to conclude that zebra mussels are clarifying waterbodies at extremely high rates (e.g., MacIsaac et al. 1992; 1999; Fahnenstiel et al. 1995; Holland et al. 1995). Although this may be the case for shallow inshore environments, deeper offshore environments need to be examined. This simple approach fails to consider (1) the physical processes that occur in these offshore environments at the spatial and temporal scales relevant to zebra mussel suspension feeding (top down processes) and (2) the potential of alternative hypotheses to explain the observed changes in water quality. It was deemed important to examine the benthic–pelagic coupling of zebra mussels in the offshore environment of the western basin of Lake Erie to ascertain whether zebra mussels are able to clarify deeper water columns.

The purpose of the present study is, therefore, to examine the degree of benthic–pelagic coupling in a zebra mussel bed located offshore in western Lake Erie.

Materials and methods

The study was conducted over an isolated elliptically shaped reef 1 km from North Harbor Island in western Lake Erie (Fig. 1). The reef measured ~ 300 by 500 m and the water depth varied from 7 to 11 m (Fig. 2). Zebra mussels were present at high densities on the reef ($\sim 7,500$ mussels m^{-2} ; $7,693 \pm 1,354$ [mean \pm SEM], $n = 3$, as determined from samples collected by SCUBA divers [J.D.A.] and ponar grabs), but negligible densities were observed on the surrounding soft, muddy sediments off the reef (11 m deep). It is important to note that this study was undertaken before

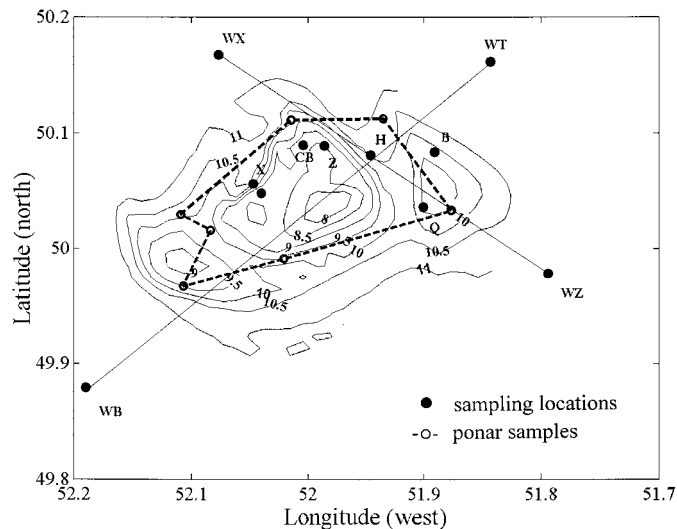


Fig. 2. Location of the sampling stations within the isolated elliptically shaped reef (~ 300 by 500 m; 7 – 11 m deep) are shown against the reef bathymetry in meters. The straight lines correspond to the 45° and 135° transects originating and terminating off the reef where zebra mussels were not found. The dotted line shows the extent of zebra mussels confirmed through ponar samples.

the onset of the colonization of soft sediments by zebra mussels (Coakley et al. 1997). All of the mussels were identified as *Dreissena polymorpha* and were present in three size classes (0.3 , 1.7 , and 2.5 cm long; Fig. 3).

An array of unattended instruments, which included four ultrasonic current meters with built-in water temperature sensors and a wave and tide recorder, was moored on the reef from 7 July to 24 August 1994 (i.e., days 188 – 235) over three sequential deployment periods (1 – 7 July to 19 July, days 188 – 200 ; 2 – 21 July to 3 August, days 202 – 215 ; and 3 – 12 August to 23 August, days 224 – 235). The current meters (EG&G model SACM-3) were oriented vertically to measure horizontal components of the velocity. They were moored at heights of 0.8 , 1.2 , 4.4 , and 5.8 m above the lake bed and were programmed to burst-sample the velocity at a rate of 2 Hz for 256 s every hour and to record one 4 -min average of the velocity and temperature every 10 min. The

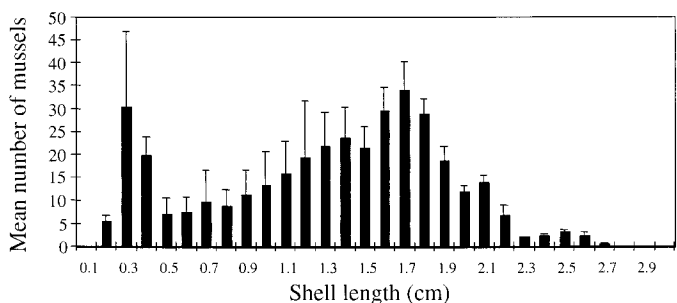


Fig. 3. Size frequency distribution of zebra mussels collected on the reef by SCUBA. The population of mussels was characterized by three size/age classes (0.3 , 1.7 , and 2.5 cm long). Population densities were estimated at $\sim 7,500$ mussels m^{-2} . This estimate is considerably lower than those made for inshore environments that are orders of magnitude higher (bar = mean; error bar = SEM; $n = 3$).

wave and tide recorder (Seadata model 365-11), which was moored on the lake bottom, was programmed to record the mean water level once every 10 min. The instruments were calibrated before and after the experiment by the National Water Research Institute Calibration Laboratory (CCIW, Burlington, Ontario). Meteorological data were obtained from a meteorological buoy installed for the experiment and, when needed to fill in gaps in coverage, from an Atmospheric Environment Service (Environment Canada) weather station off of Point Pelee (~30 km east of the experiment site).

A series of collecting stations (buoys) were established along the major axes (45° and 135° bearing) of the reef to provide two transects for our vessel to follow. Each transect began and terminated with an off-reef station ~200 m from the reef. We conducted a series of cruises from 12 July to 15 July 1994 (days 193–196), during which we sampled the seston at five heights above the bed (0.5, 1.0, 2.0, 4.0, and 8 m) at each of five stations along a transect (e.g., buoys WB, X, CB, H, and WT for the 45° transect; Fig. 2). Approximately 1 liter (1.015 liters) of the water pumped from each depth was vacuum filtered through precombusted and preweighed glass microfiber filters (GF/C; Whatman, International; nominal opening of 1.2 μm), stored on ice for transport, and stored later in a freezer until processing (within 3 weeks). The filters were dried at 60°C for 12 h and ashed at 450°C for 2 h to determine organic and inorganic components of the seston.

The total fluorescence of a 50-ml aliquot of water sampled at each height was measured using a calibrated portable fluorometer fitted for chlorophyll *a* analysis (Turner Digital Fluorometer; Model 10-AU; Turner Designs). A separate 290-ml water sample, taken at all depths at the central station of each transect, was filtered, placed in petri dishes, wrapped in aluminum foil, and stored in the dark on ice until transfer to a freezer (<1.5 h). Chlorophyll *a* was extracted from the filters in cold 90% acetone overnight, centrifuged for ~15 min at 675 g and allowed to come to room temperature (~23°C) in the dark. The fluorescence of the supernatant was measured before and after acidification with 0.003 N HCl using the fluorometer. The corrected chlorophyll *a* concentration was determined using USEPA Method 445.0 (USEPA 1992).

The ability of zebra mussels to filter lake water from the site was examined in a recirculating flow chamber (180 cm long × 17 cm wide × 3.5 cm), using the procedures described in Ackerman (1999). Mussels and 14.5 liters of lake water collected on the reef were kept at collection temperature (21–23°C) and used within 6 h of collection. Three experiments were conducted with lake water pumped from 1 m deep, and a fourth experiment was conducted with lake water pumped from 1 m above the reef. Triplicate 1-liter samples of the lake water used in the flow chamber were filtered through GF/C filters before the experiment to provide a measure of the initial seston concentration (C_0). For each experiment, 100 mussels (16.5 ± 0.4 mm long), separated from their byssal connections on rocks, were placed upright in the test section 130 cm downstream according to Ackerman (1999). The axial flow pump provided an average mid-channel flow of ~7.5 cm s⁻¹ (determined by the transport of dye), which was sufficient to maintain the seston in suspension over the relatively short experimental period (Ack-

erman 1999). Each experiment was run for ~60 min, after which time three 1-liter water samples were filtered to measure the final seston concentration (C_t). A new batch of mussels was used in each experiment. The clearance rate (CR) was determined from the following expression reviewed in Wildish and Kristmanson (1997).

$$CR = \frac{Vol}{nt} \ln \left(\frac{C_0}{C_t} \right) \quad (1)$$

Vol is the volume filtered (14.5 liters), t is time, and n is the number of mussels. The size frequency distribution of mussel length was also used in the size-based allometric model developed by Kryger and Riisgard (1988) to predict CR for each mussel batch as a comparison to Eq. 1.

Results

Water column mixing processes—The hourly averaged wind and currents at heights of 0.8 and 5.8 m for days 193–196 are presented in Fig. 4. The average wind speed was 6.7 m s⁻¹, and the predominant wind directions were to the east and southwest (Fig. 4a). The plots of current directions at depths indicate that a complex vertical velocity profile existed over the reef during the four-seston sampling days, with an average velocity of 4.4 cm s⁻¹ to the northeast, east, and north at middepth (e.g., 5.8 m above the bed; Fig. 4b) and 3.3 cm s⁻¹ to the east or west near the bed (e.g., 0.8 m above the bed; Fig. 4c). However, because of the mean hydraulic flow, the net transport at both depths was to the east-northeast with an average velocity of 1.4 cm s⁻¹. This is shown in a progressive vector plot, in which the cumulative displacements at heights of 0.8 and 5.8 m are plotted (Fig. 5). It is evident that the flow at both depths is influenced to varying degrees by (1) surface gravitational seiches, which produce the loops and sharp curves in the trajectories as the flow oscillates back and forth; (2) the mean hydraulic flow, which advects the water to the east; and (3) the wind, which causes the flow to veer to the northeast, particularly at a height of 5.8 m.

The seiching appears to be the dominant physical process governing the near-bottom currents, but it is also of importance near the surface, as seen in Fig. 6, where the time series and spectra of the water level data and the east component of the current at 5.8 m are compared. The majority of the energy in the water level fluctuations was centered at a frequency of 0.076 cph (cycles per hour), corresponding to a period of 13.2 h. This frequency corresponds closely to the predicted frequency of the lowest gravitational seiche mode: 0.071 cph or a period of 14.1 h (Hamblin 1987).

The temperature data from the current meters at heights of 0.8 and 5.8 m were used to evaluate the degree of stratification of the water column. The densimetric Froude number is a measure of the ratio of inertial to buoyancy forces.

$$F_{rd} = \frac{U}{\sqrt{g \Delta h \frac{\Delta \rho}{\rho}}} \quad (2)$$

U is the average velocity, g is the acceleration due to gravity, $\Delta \rho$ is the density difference between two points a vertical

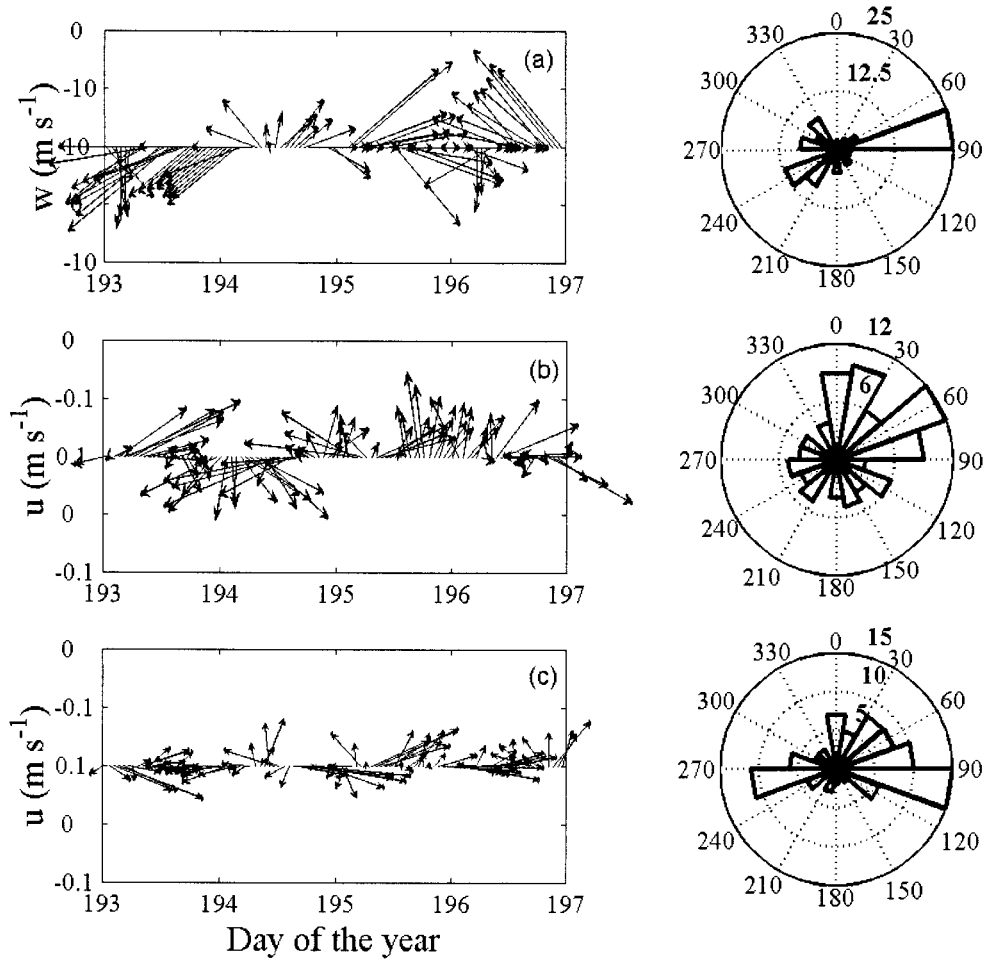


Fig. 4. Wind conditions and velocity observed within the water column during the study. Pairs of vector and rose plots showing the magnitude and direction, respectively, of the (a) wind (w), (b) current (u) at a height of 5.8 m, and (c) current (u) at a height of 0.8 m. Time is GMT.

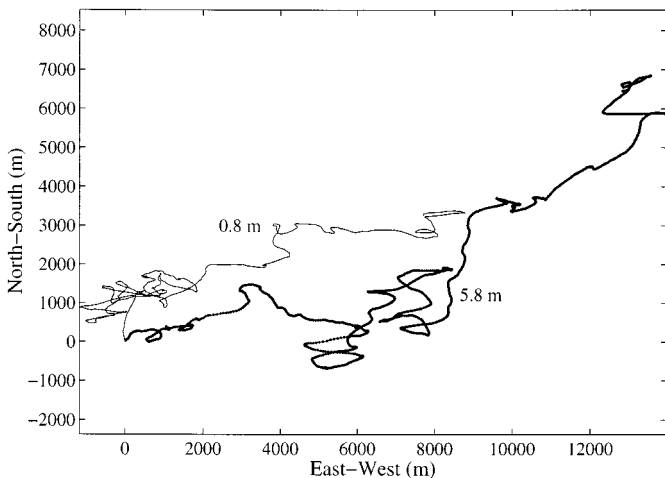


Fig. 5. A progressive vector plot of the displacement of fluid over deployment 3 for currents measured at 0.8 and 5.8 m.

distance Δh apart (i.e., $\Delta h = 5$ m in this case), and ρ is the average density. If $F_{rd} < 1$, buoyancy forces are stronger than inertial forces and internal waves continually adjust the density structure; thus, the water column remains stratified. Conversely, if $F_{rd} > 1$, inertial forces can overcome buoyancy and the water column is unstratified (Fischer et al. 1979). The densimetric Froude numbers for each of the four seston sampling periods were $F_{rd} = 0.45, 0.47, 0.74,$ and 0.47 , indicating that the water column was stratified during the sampling periods (Fig. 7). There was an irregular diurnal signal evident in the time series of F_{rd} , and the water column was typically stratified from approximately noon to late evening or early morning (local time). An evaluation of the available data indicated an $F_{rd} < 1.0$ for 76 and 44% of the time, respectively, for deployments 1 and 3. (Note that an instrument failure occurred in deployment 2.)

Estimates of the friction velocity u_* and the roughness height z_0 can be used to characterize the properties of the time-averaged velocity profile in the benthic boundary layer and to assess near-bed turbulence and, hence, mixing. Unfortunately, the boundary layer flow regime is very complex because of the influence of reef topography and roughness,

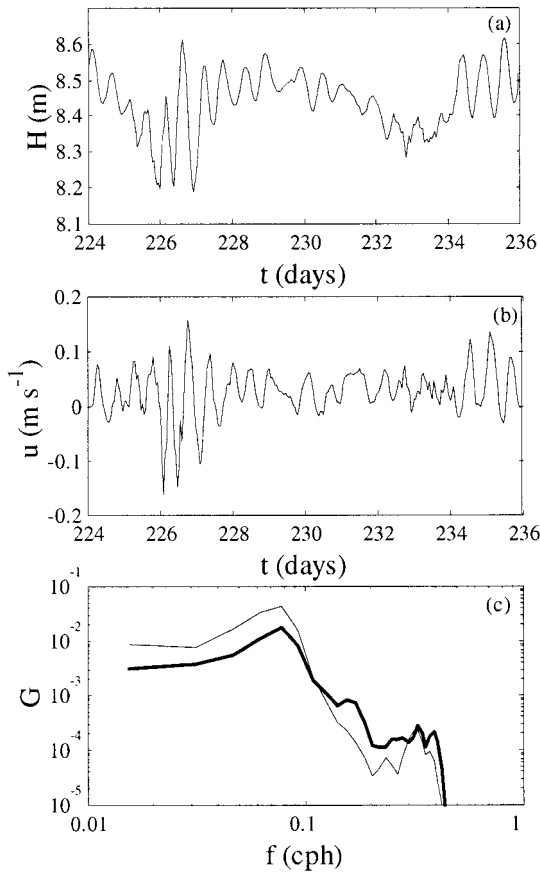


Fig. 6. (a) Water level fluctuations (H), (b) east component of the current (u) at 5.8 m, and (c) spectrum (G) of the water level (thin line) and the east component of the current (thick line) during deployment 3 (12–23 August 1994).

surface waves, internal waves, seiches, wind stress, rotation and wind-driven horizontal circulation, and the hydraulic flow in the lake system (Bedford and Abdelrhman 1987). As a result, the hydrodynamic roughness of the reef will be determined by roughness elements covering a wide range of heights, lengths, and spacings (cf., Raupach et al. 1991).

Although it is unrealistic to expect that the boundary layer flow over the reef can be modeled accurately by including all of the aforementioned forcing functions, the velocity (U) close to the boundary in a stratified water column with steady, unidirectional, fully turbulent flow over a rough boundary (i.e., hydrodynamically rough flow) may be described by

$$U = \frac{u_*}{\kappa} \left[\ln\left(\frac{z}{z_0}\right) + \frac{5z}{L_m} \right], \quad (3)$$

where κ is the von Karman coefficient ($= 0.40$), z is the height above the bed, z_0 is the roughness height, and L_m is the Monin–Obukov length (Turner 1973). This log-linear profile predicts that when the water column is stably stratified, the velocity will increase more rapidly with height above the bed than is predicted under neutral conditions (i.e., $L_m = \infty$, $\Delta\rho = 0$, and the log-linear profile is identical to

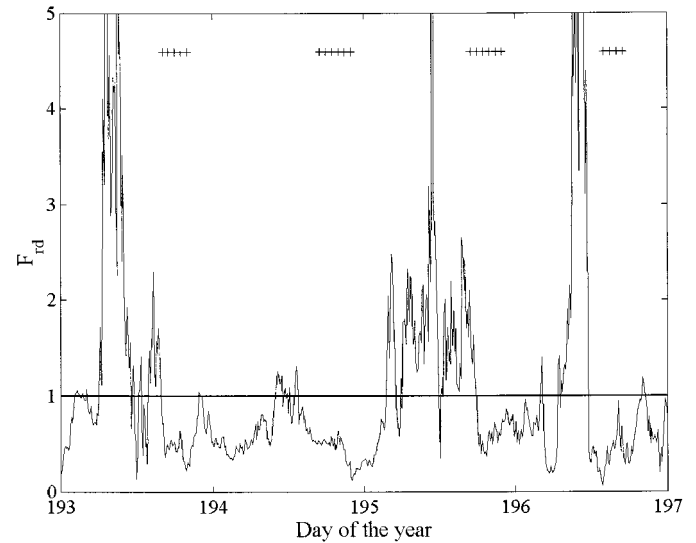


Fig. 7. The densimetric Froude number (F_{rd}) during the sestion sampling period (12–15 July 1994), where ++++ indicates the exact sestion sampling times.

the logarithmic profile—the law of the wall). The Monin–Obukov length, L_m was estimated from

$$L_m = \frac{z}{Ri}, \quad (4)$$

where Ri is the unidirectional gradient Richardson number given by (Kundu 1990)

$$Ri = \frac{g \frac{\partial \rho}{\partial z}}{\rho \left(\frac{\partial u}{\partial z} \right)^2}. \quad (5)$$

The value of Ri was estimated at $z = 0.8$ m, which was the height of the lowest current meter, and the Monin–Obukov length was then computed using Eq. 4. Values of u_* and z_0 were computed from Eq. 3 using a Levenberg–Marquardt nonlinear regression algorithm (Draper and Smith 1981) and the data from the three lowest current meters at heights of 0.8, 1.2, and 4.4 m.

The log-linear regression predicted mean values of $u_* = 0.53 \text{ cm s}^{-1}$ and $z_0 = 9.5 \text{ cm}$ (deployment 1: $u_* = 0.40 \pm 0.04 \text{ cm s}^{-1}$, $z_0 = 11 \pm 3 \text{ cm}$, $L_m = 47 \pm 15 \text{ m}$; deployment 3: $u_* = 0.65 \pm 0.05 \text{ cm s}^{-1}$, $z_0 = 8 \pm 1 \text{ cm}$, $L_m = 152 \pm 43 \text{ m}$). These results are consistent with Bedford and Abdelrhman's (1987) report of u_* ranging between 0.25 and 1 cm s^{-1} in Lake Erie prior to the zebra mussel invasion and with estimates made using the law of the wall (not shown). For perspective, a z_0 of 9.5 cm corresponds to a drag coefficient referenced to the mean velocity 100 cm above the bed equal to 2.9×10^{-2} (Gross and Nowell 1983). It should be noted that only 1.5–1.7% of the observed velocity profiles met the selection criteria, and the remaining data were discarded because (1) the velocity data did not increase monotonically with height above the bed or the directions of the velocity at the three heights were not within 0.4 radians of

Table 1. Summary of the transect data. The magnitude (U) and direction (U_{dir}) of the velocity measured at 0.8 m above the bottom, wind speed (W), and direction (W_{dir}) are presented in Fig. 4. The boat bearing and category (downstream transects in which the near-bottom flow was approximately parallel to the transect bearing [1 for 45°, 3 for 135° transects]; cross-stream transects, in which the near-bottom flow was approximately orthogonal to the transect bearing [2 for 45°, 4 for 135° transects]) with respect to U_{dir} is provided, along with the measured chlorophyll a (via in situ fluorescence) and organic and inorganic seston components determined from water samples pumped from various heights above the reef. The mean \pm standard error ($n = 25$) is presented.

Local time (h)	Transect ID-bearing-category	U (cm s ⁻¹)	U_{dir}	W (m s ⁻¹)	W_{dir}	Chlorophyll a ($\mu\text{g L}^{-1}$)	Organic seston (mg L ⁻¹)	Inorganic seston (mg L ⁻¹)
12 Jul 94								
1200–1344	A-45°-1	0.6	257°	7.5	210°	1.38 \pm 0.12	1.09 \pm 0.23	1.60 \pm 0.22
1425–1540	B-45°-2	2.2	272°	5.7	220°	1.48 \pm 0.20	1.15 \pm 0.10	1.96 \pm 0.20
13 Jul 94								
1220–1355	C-45°-2	2.9	98°	4.4	80°	1.43 \pm 0.15	1.07 \pm 0.10	1.34 \pm 0.25
1510–1610	D-135°-3	9.1	107°	4.6	90°	1.51 \pm 0.14	1.14 \pm 0.19	1.34 \pm 0.18
1623–1719	E-45°-2	6.7	108°	5.1	90°	1.80 \pm 0.20	1.10 \pm 0.12	1.31 \pm 0.28
1731–1822	F-135°-4	3.8	188°	4.1	120°	1.87 \pm 0.20	1.16 \pm 0.14	0.98 \pm 0.22
14 Jul 94								
1303–1407	G-135°-4	4.4	34°	7.7	90°	1.09 \pm 0.15	1.07 \pm 0.13	1.29 \pm 0.21
1502–1705	H-135°-4	3.9	86°	7.4	90°	1.29 \pm 0.14	1.17 \pm 0.28	1.20 \pm 0.16
1720–1817	I-45°-2	6.5	91°	8.7	90°	1.94 \pm 0.19	1.34 \pm 0.20	1.36 \pm 0.15
15 Jul 94								
1016–1103	J-45°-2	1.4	285°	7.2	280°	1.89 \pm 0.13	1.32 \pm 0.13	1.41 \pm 0.13
1114–1213	K-35°-3	1.9	293°	7.7	180°	1.79 \pm 0.17	1.27 \pm 0.16	1.38 \pm 0.16

each other and thus not unidirectional ($\sim 84\%$); (2) the correlation coefficient of the velocity profile was <0.997 , indicating that the uncertainty in u_* estimates were $>30\%$ at the 90% confidence level (Drake et al. 1992) ($\sim 13\%$); and (3) the observed velocities were less than the 1 cm s^{-1} resolution of the current meters ($<1\%$). It is evident that the simple boundary layer model described by Eq. 3 only provides an accurate description of the flow over the reef a

small percentage of the time. This is not unexpected because the flow over the reef was complex due to the competing influences of the two dominant forcing functions: surface gravitational seiching and wind-driven currents.

Water column seston sampling—Each water sampling transect was completed in 1–2 h (i.e., 25 seston samples = five heights \times five stations; Table 1). A total of 11 transects were sampled from 12 to 15 July 1994, providing 55 water column profiles or 275 seston samples. The seston data were separated into organic and inorganic components, as well as chlorophyll a concentration based on a regression of total fluorescence versus extracted chlorophyll a . The least squares fit of our data indicated that Total Fluorescence = $(0.55 \pm 0.05) \times \text{Chlorophyll } a - (0.05 \pm 0.06)$ ($r^2 = 0.69$, $n = 68$, $P < 0.001$). The wind conditions may have influenced the seston data sampled in each transect (Table 1). For example, the average chlorophyll a and organic seston concentration increased from 12 to 15 July 1994, whereas the inorganic seston decreased significantly between 12 and 13–14 July 1994 ($F_{(3,7)} = 5.89$, $P = 0.025$) during a period of reduced wind speed (Table 1).

The data were initially separated into on- and off-reef stations to explore for potential differences due to zebra mussel feeding activities. In general, profiles of chlorophyll a and organic seston concentration tended to increase with height above the bottom, both on and off the reef (33 and 22 samples per depth, respectively; Fig. 8). On-reef stations tended to have lower chlorophyll a and organic seston concentrations, especially near the bottom, but none of these trends were found to be statistically significant. However, inorganic seston concentration tended to increase toward the bottom. A relative decrease in inorganic seston concentration was

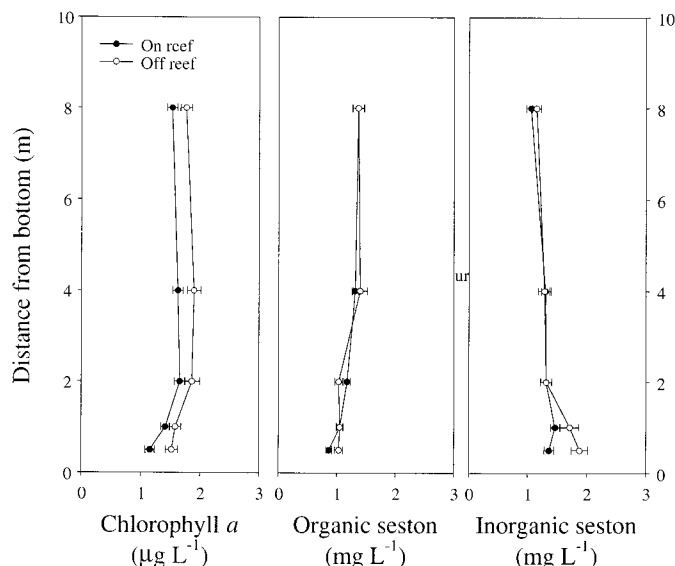


Fig. 8. Profiles of chlorophyll a and organic and inorganic seston concentrations with height above the bottom for on- and off-reef sampling stations (33 and 22 samples per height, respectively). The mean value and standard error bars are presented.

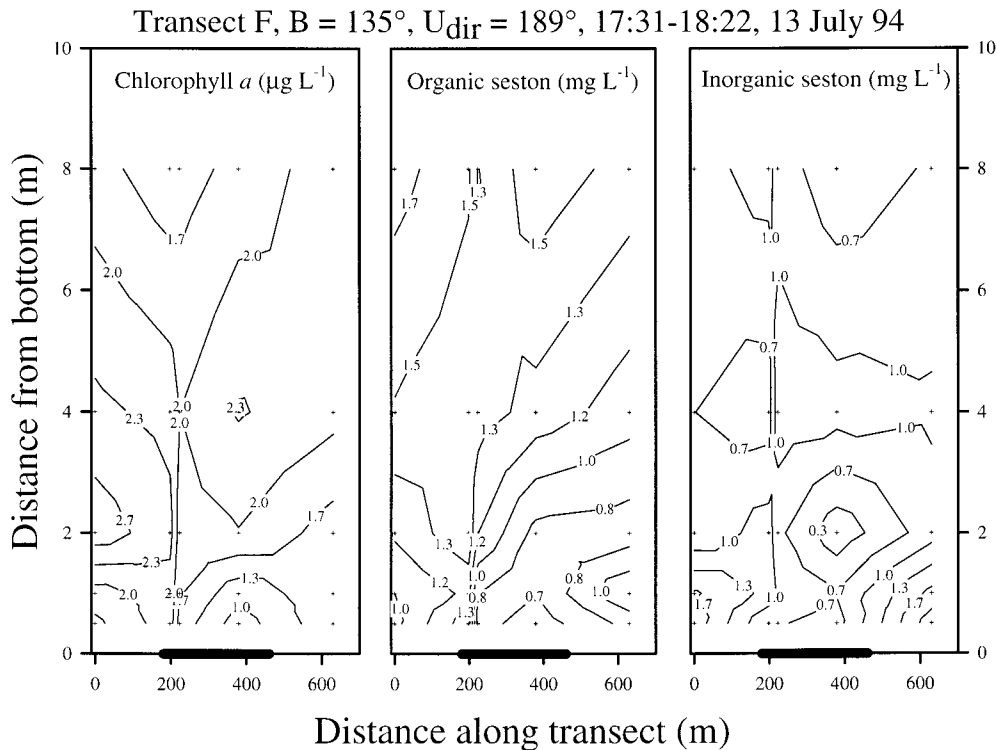


Fig. 9. Contours of chlorophyll *a*, organic seston, and inorganic seston components measured at 25 sampling locations (five heights at five distances indicated by +) along profiling transect F on 13 July 1994. The direction of the water currents measured at a height of 0.8 m were approximately orthogonal to the direction of the transect (i.e., cross-stream; see Table 1 for details). The extent of the zebra mussel-covered reef, which is surrounded by soft sediments, is indicated by the thick line on the abscissa.

observed immediately above the reef, and this was significantly lower ($P < 0.05$) than the inorganic seston concentrations measured off the reef at a height of 0.5 m.

An analysis that included the spatial coordinates of the sampling locations was undertaken on the seston data. The data contours of the chlorophyll *a*, organic seston, and inorganic seston components are provided for transect F on 13 July 1994 (Fig. 9). The 25 sampling locations (five depths \times five stations) are indicated by the + symbols, along with the extent of the reef, as indicated by the thick line on the abscissa. The chlorophyll *a* concentration contours showed a trend to lower concentrations at greater distances along the transect (i.e., the abscissa of Fig. 9). The chlorophyll *a* contours ranged from 1.7 to 2.0 $\mu\text{g L}^{-1}$ (5 to 8 m above the reef) to 2.3 $\mu\text{g L}^{-1}$ (2 to 5 m above the reef) and decreased to $<1 \mu\text{g L}^{-1}$ closer to the reef. The lowest concentrations were centered at a distance of 380 m and a height of 0.5 m directly over the reef. The organic seston concentrations exhibited similar trends over the reef; however, the organic seston concentrations were more uniform (i.e., 1.3–1.7 mg L^{-1}) within the water column. The lowest organic seston concentrations ($<0.7 \text{mg L}^{-1}$) were centered at the same location as those for chlorophyll *a*, i.e., 380 m. The inorganic seston concentrations were similar as well. The contours varied from 0.7 to 1.0 mg L^{-1} within the water column at 3–8 m above the reef and declined to 0.3 mg L^{-1} at a height of 2 m. Inorganic seston concentrations immediately above the

reef were at a minimum of 0.7 mg L^{-1} at a distance of 380 m. Higher inorganic seston concentrations (e.g., 1.7–2.1 mg L^{-1}) were observed within 1 m above the lake bed immediately above the soft sediments on either side of the reef.

A statistical analysis was undertaken for boat transect bearings of 45° (e.g., A, B, C, E, I, and J; Fig. 10) and 135° (e.g., D, F, G, H, and K; Fig. 11) to determine the statistical significance of the vertical gradients in seston constituents above the reef and off of the reef. These analyses involved the computation of the standard deviate within each transect (i.e., $z = [x - \mu]/\sigma$, where z is the standard deviate, x is the observation, and μ and σ are the mean and standard deviation measured within a transect). The standard deviates were averaged across the same water column locations (i.e., distance and height) and contoured (Fig. 10, 11). In this analysis, regions of average concentration have standard deviates of zero; those of higher concentration have positive values, whereas those of lower concentration have negative values. Standard deviates of magnitude ≥ 1.96 can be considered statistically significant at $P < 0.05$ (e.g., Rohlf and Sokal 1995). Significantly lower standard deviates for chlorophyll *a* directly above the reef were observed for nine of the 11 transects undertaken on the 4-d period. Significantly lower standard deviates for organic seston were found on transects B and J on 12 and 15 July 1994. Only one of the 11 transects (B) had significantly lower standard deviate values for inorganic seston directly above the reef.

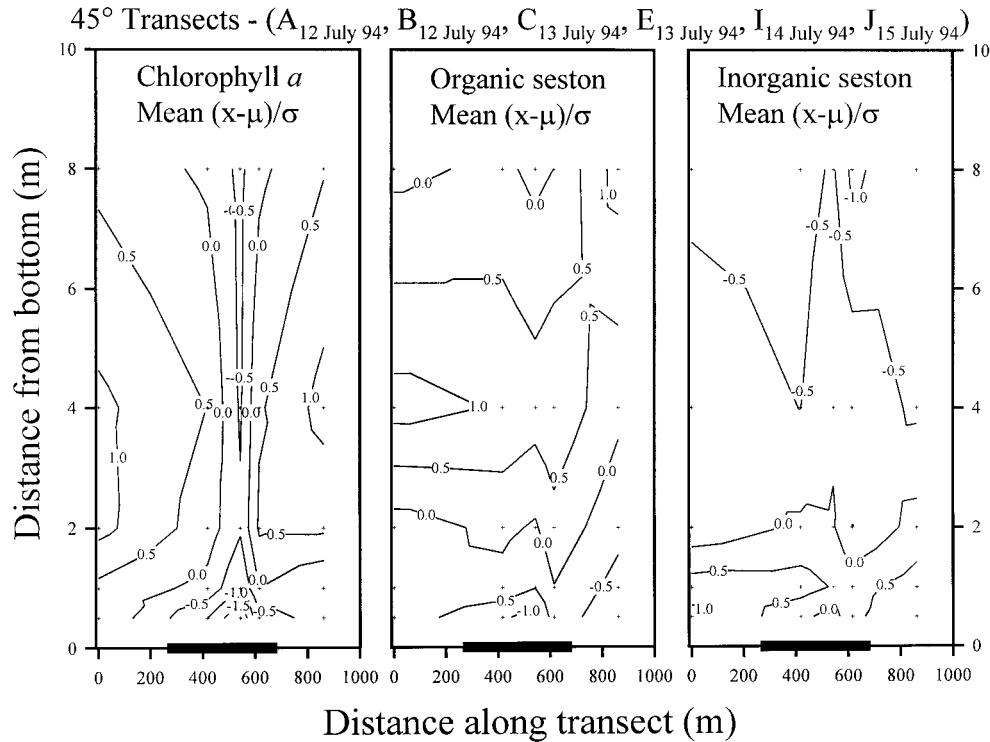


Fig. 10. Contours of the mean standard deviates of chlorophyll *a*, organic seston, and inorganic seston components measured on six 45° transects (A, B, C, E, I, and J) between 12 and 15 July 1994 (see Table 1 for details). The standard deviates were determined within each transect ($(x - \mu)/\sigma$, where x is the observation and μ and σ are the mean and standard deviation measured within a transect, respectively) and ensemble averaged across sampling locations. Standard deviates greater than ± 1.96 would be significant at $P < 0.05$. The sampling locations are indicated by +. The extent of the zebra mussel-covered reef, which is surrounded by soft sediments, is indicated by the thick line on the abscissa.

The standard deviate contours for chlorophyll *a* concentrations resembled those observed on a single transect (compare Fig. 9 with Figs. 10, 11; note the different bearings of the transects, which are presented in Fig. 2). The chlorophyll *a* concentrations in the water column were relatively uniform, with standard deviate values of 0.0 to 1.0 from 2 to 5 m above the reef. There was a sharp decline in average standard deviate values from 0.0 at a height of 2 m to -1.5 at 0.5 m above the reef at a distance of 580 m for 45° transects (Fig. 10) and -1.3 at 0.5 m above the reef at a distance of 300 m for 135° transects (Fig. 11). Although there is an obvious gradient in chlorophyll *a* concentration toward the reef, the lack of significance in these contour values may be related to the averaging process, since nine of the 11 transects had significantly lower standard deviates.

The standard deviate values for organic seston concentration were reasonably consistent with those for chlorophyll *a* and transect F. Values ranged from 0.5 to 1.0 at a height of 2–8 m, with a maximum of 1.0 at 4 m for 45° transects (Fig. 10) and a maximum of 1.3 at 7.5 m for 135° transects (Fig. 11). In general, the average value of ~ 0 (i.e., the mean) was observed at a height of 2 m above the bottom. The standard deviate values declined from 0.0 at a height of 2 m to -1.0 at 0.5 m immediately above the reef at a distance of 580 m for the 45° transects (Fig. 10) and -1.2 at 0.5 m immediately

above the reef at a distance of 380 m for the 135° transects (Fig. 11). The standard deviate values for inorganic seston concentration increased from approximately -0.7 at a height of 8 m to ~ 0 at 2 m. A minimum of 0.0 was observed at a distance of 580 m and a height of 0.5 m for the 45° transects (Fig. 10), whereas a minimum of -0.3 was observed at 0.5 m immediately above the reef at a distance of 380 m for the 135° transects (Fig. 11), as was the case for chlorophyll *a* and organic seston. In general, the magnitudes of the declines in the chlorophyll *a* and seston components directly over the reef were stronger for the 45° transects than for the 135° transects (Fig. 10 versus 11).

An additional contour plot is provided for a subset of three 45° transects (C, E, and I; Fig. 12), in which the approaching velocity direction was similar (i.e., approximately east), in an attempt to examine the consistency of the seston components. The standard deviate contours for chlorophyll *a* concentrations resembled those described above for the larger sample (Fig. 10), but there was a marked and significant decline (i.e., ≥ 1.96 ; $P < 0.05$) in average standard deviate values from 0.0 at a height of 2 m to -2.0 at 0.5 m above the reef at a distance of 580 m. The standard deviate values for organic seston concentration were reasonably consistent with those for chlorophyll *a*, although they declined from 0.0 at a height of 2 m to -1.5 at 0.5 m immediately above

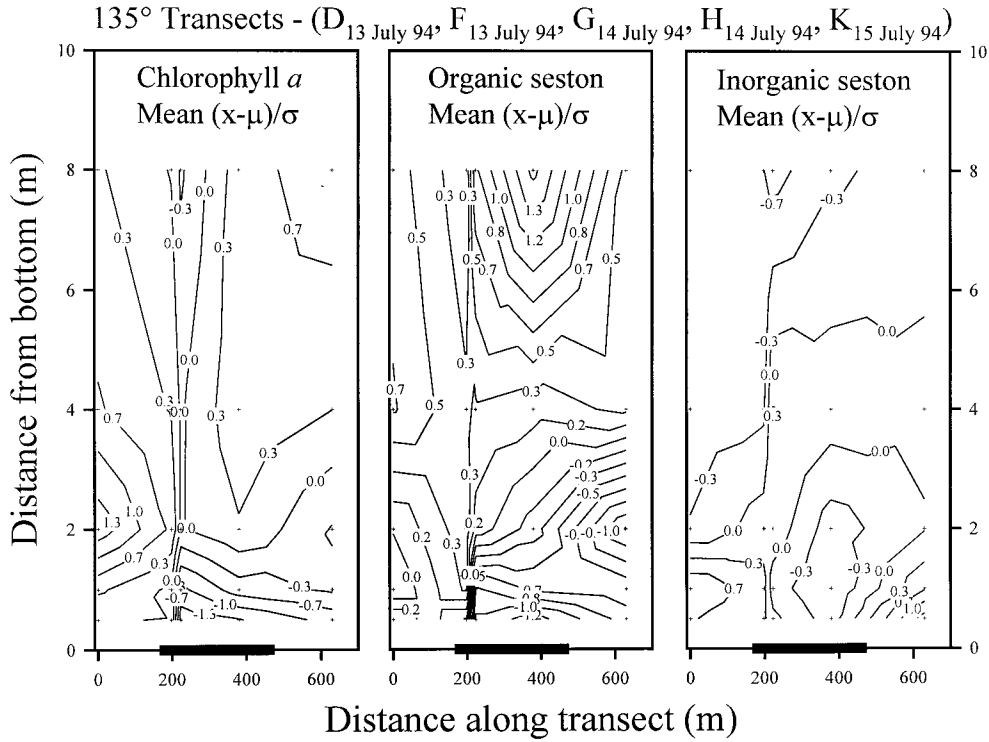


Fig. 11. Contours of the mean standard deviates of chlorophyll *a*, organic seston, and inorganic seston components measured on five 135° transects (D, F, G, H, and K) between 13 and 15 July 1994 (see Table 1 for details). Analysis and symbols as in Fig. 10.

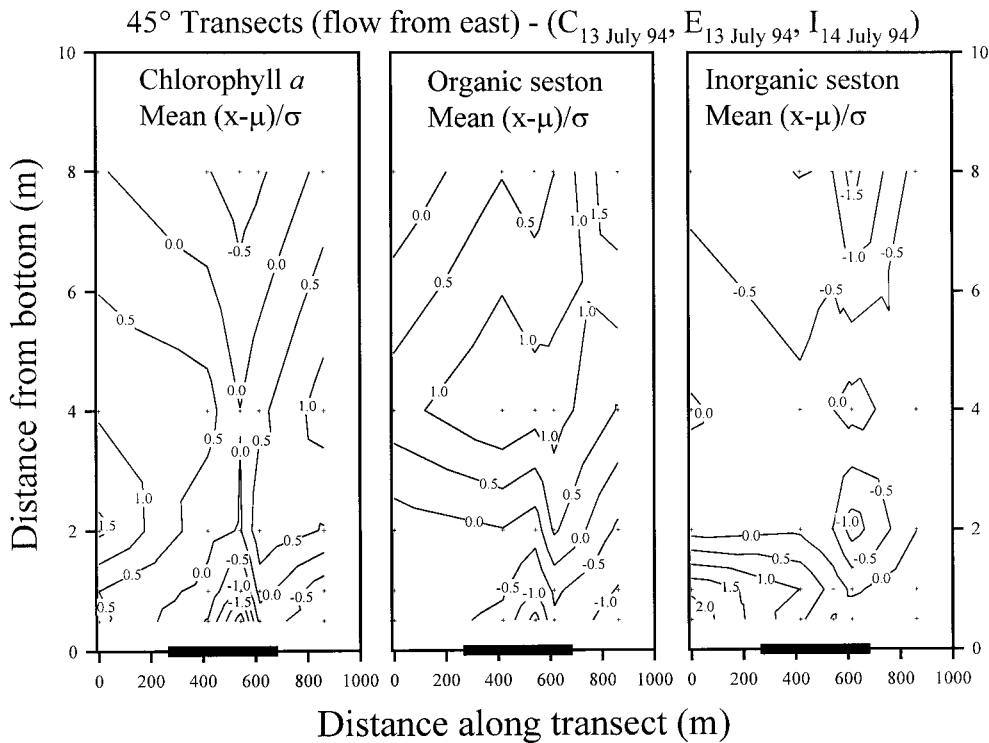


Fig. 12. Contours of the mean standard deviates of chlorophyll *a*, organic seston, and inorganic seston components measured on three 45° transects (C, E, and I) between 13 and 14 July 1994, in which the approaching flow was to the east (see Table 1 for details). Analysis and symbols as in Fig. 10.

the reef at a distance of 580 m, which was not significant ($P < 0.13$). The standard deviate values for inorganic seston were similar to that found in Fig. 10.

Zebra mussel clearance of natural seston—The potential effect of zebra mussels on the water column seston was examined in four suspension-feeding experiments conducted in a recirculating flow chamber using lake water at 21.5–22.5°C. The initial seston concentrations in the experiments were relatively high, averaging $2.55 \pm 0.06 \text{ mg L}^{-1}$ (mean \pm SE; $n = 4$) in total seston, and the proportions were similar for organic and inorganic seston fractions ($1.2 \pm 0.1 \text{ mg L}^{-1}$ and $1.3 \pm 0.1 \text{ mg L}^{-1}$, respectively). The water pumped from a height of 1.0 m above the reef had a lower ratio of organic/inorganic fractions (0.42 versus 1.2 ± 0.2 for the remaining three experiments), as would be expected from the data presented in Fig. 8. On average, the mussels removed $\sim 40\%$ of the total seston in the chamber ($C_i = 1.5 \pm 0.1 \text{ mg L}^{-1}$), with a smaller reduction in organic than inorganic fractions ($C_i = 0.8 \pm 0.1 \text{ mg L}^{-1}$ and $C_i = 0.64 \pm 0.07 \text{ mg L}^{-1}$, respectively). This corresponded to an average clearance rate of $87 \pm 22 \text{ ml mussel}^{-1} \text{ h}^{-1}$ of total seston. Mussels tended to clear less of the organic than inorganic fractions ($59 \pm 24 \text{ ml mussel}^{-1} \text{ h}^{-1}$ and $110 \pm 44 \text{ ml mussel}^{-1} \text{ h}^{-1}$, respectively).

Discussion

Benthic–pelagic coupling over the reef—A comparison of water column chlorophyll *a* and seston did not reveal statistically significant differences between stations on and off of a zebra mussel-dominated reef, except in the case of inorganic seston at 0.5 m above the lake bed (Fig. 8). This latter difference, where there is more inorganic seston off the reef, may be due to the entrainment of sediments in the flow near the bottom and the possible pumping of the softer sediments by the submersible pump. Concentration gradients in chlorophyll *a* and organic seston were, however, observed between heights of 0 and 2 m, both on and off the reef. Although the gradient was steeper on the reef compared to off the reef, it was not found to be significantly different. If zebra mussel feeding effects were strong, one would expect to see steeper gradients on the reef and stronger differences in the concentrations and the gradients between on- and off-reef stations. However, when the horizontal spatial information was incorporated in the analysis, water column contours revealed the effects of zebra mussel feeding. Although other sinks for seston are present in the field (e.g., zooplankton grazers, settling of seston), it is difficult to envision a scenario whereby there would be spatial differences in these other sinks corresponding in the same manner as the zebra mussels on the reef.

It is also important to note that our observations can be considered reliable because chlorophyll *a* and seston concentrations were measured by different techniques (i.e., fluorometry of water samples, and mass of material filtered from water samples). The consistency and statistical significance of the lowest concentrations being nearest the bottom (i.e., 0.5 m above the lake bed) is noteworthy given the different sampling dates and range of environmental conditions (Table

1). Therefore, it is reasonable to conclude that there is a sink for seston on the bottom.

The concentration boundary layer above the reef is the consequence of zebra mussel feeding. The strength of the concentration boundary layer will vary temporally and spatially with the currents, location on the reef, and response of the zebra mussels. This signal would be strong if the water column was stratified, thus limiting the vertical exchange of water. As determined above, the measured densimetric Froude number (F_{rd}) was less than unity during the seston sampling periods, indicating that the water column was stratified (Fig. 7). Importantly, stratification was observed $\sim 60\%$ of the time and usually occurred from noon to late evening or early morning. Similar gradients in chlorophyll *a* were observed within ~ 1 m of the lake bottom in shallower locations in Western Lake Erie during periods of stratification (MacIsaac et al. 1992). Assuming that the results presented above are representative of summer conditions, it is likely that stratification occurred $\sim 60\%$ of the time during the entire summer of 1994.

Direct measurements of the vertical mixing (e.g., turbulent vertical velocity) were not possible with the available instrumentation, but inferences can be drawn from the boundary layer observations. Koseff et al. (1993) used a numerical model to show that in shallow estuaries, stratification removed the connection between benthic suspension feeders and the near-surface phytoplankton biomass by decreasing the vertical transport of the phytoplankton.

The approximate time it would take a population of benthic suspension feeders to deplete a water column of depth H of phytoplankton is given by

$$\tau_{\text{graze}} = \frac{H}{\alpha}, \quad (6)$$

where τ_{graze} is the timescale for benthic grazing and α is the areal clearance rate (Koseff et al. 1993). Given the mussel density on the reef ($\sim 7,500 \text{ mussels m}^{-2}$) and the average clearance rate from the flume experiments ($\sim 90 \text{ ml mussel}^{-1} \text{ h}^{-1}$) gives $\alpha = 0.675 \text{ m}^3 \text{ h}^{-1} \text{ m}^{-2}$. Using a depth $H = 8$ m provides a timescale for benthic grazing of $\tau_{\text{graze}} = 11.9$ hours.

The approximate time it would take for the turbulence to mix the phytoplankton over depth H is given by

$$\tau_{\text{diff}} = \frac{H^2}{\epsilon_z}, \quad (7)$$

where τ_{diff} is the diffusive timescale and ϵ_z is the vertical turbulent diffusion coefficient. At times when the water column above the reef is stably stratified, the vertical mixing will be inhibited, and the magnitude of the vertical turbulent diffusion coefficient will be reduced according to the Munk and Anderson (1948) expression given by

$$\epsilon_z = \epsilon_0(1 + 3.33\text{Ri})^{-3/2} = \epsilon_0\beta, \quad (8)$$

where ϵ_0 is the value of ϵ_z for neutral stability given by (Fischer et al. 1979)

$$\epsilon_0 = 0.067Hu_* \quad (9)$$

It was estimated that, on average, ϵ_z was reduced by 44%

during deployment 1 and 20% during deployment 3 (i.e., average $\beta = 0.56$ and 0.80 , respectively). The value of β during the seston sampling periods was 0.60 , 0.63 , 0.56 , and 0.66 , respectively, indicating that, on average, ϵ_z was reduced by $\sim 40\%$ at these times.

Applying Eq. 9 under stably stratified conditions using $u_* = 0.0053 \text{ m s}^{-1}$ and $\beta = 0.60$ for the seston sampling periods in Eq. 8 gives $\epsilon_z = 0.0017 \text{ m}^2 \text{ s}^{-1}$. Then Eq. 7 predicts that $\tau_{\text{diff}} = 10.4 \text{ h}$ for the stratified conditions that occurred during the seston sampling periods. As a comparison, the diffusive timescale for neutral conditions was estimated by computing an average value of u_* using the law of the wall and linear regression for times when F_{rd} was >1.0 (not shown). Using the average u_* of 0.0073 m s^{-1} , Eq. 9 predicts $\epsilon_0 = 0.0041 \text{ m}^2 \text{ s}^{-1}$, and consequently, Eq. 7 provides a τ_{diff} of 4.5 h .

These scaling arguments indicate that when there is no significant stratification τ_{diff} is approximately two and a half times smaller than τ_{graze} . During these time periods, the vertical mixing will be so strong relative to benthic grazing that the mussels have access to more of the water column, and only a relatively weak concentration boundary layer would be expected to form near the bed. During the seston sampling periods, the diffusive timescale was predicted to increase to 10.4 h , which is comparable to 11.9 h , the predicted value of the timescale for benthic grazing. When the two timescales are equal, the strength of vertical mixing and benthic grazing is approximately equal; therefore, a stronger concentration boundary layer should form above the bed. As noted above, concentration boundary layers were observed on all 4 d of seston sampling. Interestingly, although we found that concentration boundary layers can form above benthic grazers in the presence of semidiurnal stratification, Lucas et al. (1998) recently demonstrated that periodic stratification does not increase the probability of phytoplankton blooms.

Although a concentration gradient was observed over the reef, it was relatively weak, and it was not present over the entire reef (see Figs. 9–12). Moreover, other factors, such as jets emanating from bivalve exhalant siphons, are known to lead to refiltration in benthic bivalves and influence the near-bottom mixing (Monismith et al. 1990; O’Riordan et al. 1995). Laboratory experiments showed that the maximum refiltration n_{max} is given by

$$n_{\text{max}} \approx 2.5 \frac{d_0}{S}, \quad (10)$$

where d_0 is the exhalant siphon diameter and S is the average distance between the siphons (O’Riordan et al. 1995). For zebra mussels of the principle size on the reef, d_0 is $\sim 2 \text{ mm}$ (MacIsaac et al. 1992) and S is $\sim 12 \text{ mm}$, given a density of $\sim 7,500 \text{ mussels m}^{-2}$. Equation 10 predicts $n_{\text{max}} = 0.42$ for this zebra mussel reef. In other words, mussels upstream are predicted to have previously filtered $\sim 40\%$ of the water that the mussels are filtering, which is an upper limit, given that the orientation of zebra mussel siphons is not likely to be as uniform in space, nor would they be constantly pumping, as in the laboratory model. Regardless, this value is consistent with recent estimates of refiltration made by Yu and Culver

(1999). The refiltration of bottom water combined with the limited vertical mixing of the water column due to stratification would restrict the suspension-feeding signal to the region immediately above the reef and, thus, lead to a more pronounced concentration boundary layer.

Potential effects of zebra mussels—The potential effects of zebra mussels on the water column were examined in the clearance rate experiments. Results indicate that zebra mussels could remove up to 40% of the total seston in the flow chamber. The $\sim 90 \text{ ml mussel}^{-1} \text{ h}^{-1}$ clearance rate falls within the range of observations obtained for *Dreissena polymorpha* of this size (note that reported rates vary over two orders of magnitude; Ackerman 1999). This value was $\sim 40\%$ lower than the $157 \text{ ml mussel}^{-1} \text{ h}^{-1}$ rate predicted for the mussels in the flow chamber using the allometric model developed by Kryger and Riisgard (1988), and is opposite to what Ackerman (1999) found using a *Chlorella* monoculture in the same chamber at comparable temperatures. Moreover, it is also lower than what would be expected given the enhancement of clearance rates by velocity noted by Ackerman (1999; also see Wildish and Kristman 1997). Unfortunately, most of these comparative data were based on observations made using algal monocultures added to filtered lake water (see review in Ackerman 1999). Lake water is more complex in terms of the algal and other constituents, and the concentrations of total seston may also exceed the 2 mg L^{-1} incipient threshold seston concentration for *D. polymorpha* when clearance rates decline exponentially (Sprung and Rose 1988; Reeders and Bij de Vaate 1990). This is supported by findings in Saginaw Bay, Lake Huron, where lower clearance rates were observed in the inner bay compared to the outer bay, even though seston concentrations were higher in the inner bay (Fanslow et al. 1995). It is reasonable, therefore, to expect clearance rates that are lower than predicted values given the use of natural lake water and the initial seston concentrations that were greater than the incipient threshold seston concentration (cf. Butman et al. 1994).

Results from this study provide an opportunity to estimate the reef clearance rate for the sampling transects using Eq. 1. The direction of the water at a height of 0.8 m was used to determine where the water first contacted the reef. The distance from this point to the region of minimum concentration observed in the contours (e.g., Fig. 9), provided the water path length (d) for further calculations. The volume (Vol) was determined as the water within a 1-m width and a 1-m height (i.e., corresponding to the height of the concentration boundary layer) along the path d . The number of mussels (n) was determined as the product of the area (i.e., $d \text{ m}^2$) and the mussel density ($\sim 7,500 \text{ mussels m}^{-2}$). The initial seston concentration (C_0) was taken at the off-reef station, and the final seston concentration (C_f) was taken at the sampling station closest to the minimum. Time (t) was calculated from the quotient of d and the water velocity measured at a height of 0.8 m . The results for the sampling transects varied according to transect and the seston component analyzed (i.e., total seston and organic and inorganic seston fractions). Average clearance rates of $107 \pm 46 \text{ ml mussel}^{-1} \text{ h}^{-1}$ for chlorophyll *a* and $98 \pm 33 \text{ ml mussel}^{-1} \text{ h}^{-1}$

of total seston were estimated. As with the flume experiments, mussels tended to clear less of the organic than inorganic fractions (76 ± 21 ml mussel⁻¹ h⁻¹ and 113 ± 40 ml mussel⁻¹ h⁻¹, respectively), and these results were ~40% lower than the 126 ml mussel⁻¹ h⁻¹ rate predicted from the mussel size distribution on the reef (i.e., Fig. 3) using the allometric empirical model developed by Kryger and Riisgard (1988).

To assess the potential bias associated with single-point estimates (e.g., Fréchette et al. 1993), we repeated our analysis using initial and final seston concentrations based on the integration of the bottom two sampling locations (i.e., 0.5 and 1.0 m). We assumed that the concentration at the bed was 50% of the value at 0.5 m, and then we integrated from the bed to a height of 1.25 m. The results were similar to those reported above, although the estimated clearance rates were ~20% lower. The average clearance rate for chlorophyll *a* was 88 ± 33 ml mussel⁻¹ h⁻¹, whereas 81 ± 29 ml mussel⁻¹ h⁻¹ was estimated for total seston. There was a higher clearance of inorganic than organic fractions (96 ± 35 ml mussel⁻¹ h⁻¹ and 59 ± 19 ml mussel⁻¹ h⁻¹, respectively).

These estimates of the effects of zebra mussel are surprisingly similar given the very different techniques used in the field and in the laboratory. This suggests that our flow chamber results, which indicate that zebra mussel feeding rates are lower than those predicted by other studies (see above), are sound. Furthermore, the positive association of velocity during the transect and clearance rate estimates ($r^2 = 0.57, 0.44,$ and 0.56 for total seston, and organic and inorganic seston fractions, respectively) supports a similar finding of a positive effect of velocity on the suspension feeding of zebra mussels and other benthic bivalves (Ackerman 1999).

Clearance rate estimates from the laboratory are often used to model the effects of benthic grazers on aquatic ecosystems. A common approach is to use a simple reactor model (cf. τ_{graze}), which estimates the grazing effect from the quotient of the volume of the waterbody and the areal clearance rate (e.g., Reeders et al. 1989). Unfortunately, this approach ignores (1) water column physical processes (e.g., stratification, benthic boundary layer flow, and diffusion), (2) the effect of field conditions (e.g., velocity and complexities of natural seston) on benthic clearance rates, and (3) the spatial heterogeneity of suitable substrates. The applicability of this model even to shallow well-mixed environments is questionable (e.g., in 3-m mean depth in Lake St. Clair; Hebert et al. 1991; Yamamuro and Koike 1994), but its application in deeper offshore environments will almost certainly lead to high estimates of benthic grazing.

The observation of an algal concentration boundary layer over the mussel bed is evidence that the simple reactor model is an oversimplification, as are other models that ignore stratification (MacIsaac et al. 1999).

Another factor that is ignored in these assessments is seasonal differences in mixing and ecophysiology that could influence the effects of benthic grazers. One could model seasonal differences based on expectations that the effect of benthic grazers would be greater during periods of higher mixing (e.g., fall and spring) and warmer water temperatures

when clearance rates are higher (e.g., summer). Unfortunately, this assessment is problematic for zebra mussels because (1) both positive and negative responses to increasing temperature up to a maximum of 20–26°C have been reported by different authors (see Fisher et al. 1993; Lei et al. 1996) and (2) there is a paucity of water column mixing data in other seasons. This is an area that should be addressed in the future through direct measurements in the field.

There can be little doubt that the introduction of large numbers of suspension feeders into Lake Erie has affected the water quality (Makarewicz et al. 1999, 2000; Nicholls et al. 1999). However, several factors may have contributed to the conventional wisdom that zebra mussels are the only possible explanation for the clarification of Lake Erie. First, previous field studies have tended to concentrate on near-shore regions, where the effect of zebra mussels will be greater because of their high population density and strong vertical mixing. Second, the application of simple reactor models to the entire basin will overestimate the effect of zebra mussel suspension feeding (e.g., ≤ 18.8 times daily [MacIsaac et al. 1992]; also see criticisms in Yu and Culver [1999] and Makarewicz et al. [1999]). Plausible additional factors that contribute to water quality changes include (1) the significant decline in phytoplankton biomass and change in species composition that occurred prior to the introduction of zebra mussels (Makarewicz 1993), which was coincident with phosphorus abatement strategies (Schelske and Hodell 1995), and (2) grazing by native zooplankton (Wu and Culver 1991).

Given these and other findings, we recommend that the proposed role of zebra mussels in the clarification of Lake Erie be investigated further.

References

- ACKERMAN, J. D. 1999. The effect of velocity on the filter feeding of zebra mussels (*Dreissena polymorpha* and *D. bugensis*): Implications for trophic dynamics. *Can. J. Fish. Aquat. Sci.* **56**: 1551–1561.
- BEDFORD, K. W., AND M. ABDELRHMAN. 1987. Analytical and experimental studies of the benthic boundary layer and their applicability to near-bottom transport in Lake Erie. *J. Great Lakes Res.* **13**: 628–648.
- BUTMAN, C. A., M. FRÉCHETTE, AND W. R. GEYER. 1994. Flume experiments on food supply to the blue mussel *Mytilus edulis* L. as a function of boundary layer flow. *Limnol. Oceanogr.* **39**: 1755–1768.
- CLOERN, J. E. 1991. Tidal stirring and phytoplankton bloom dynamics in an estuary. *J. Mar. Res.* **49**: 203–221.
- COAKLEY, J. P., G. L. BROWN, S. E. IOANNOU, AND M. N. CHARLTON. 1997. Colonization patterns and densities of zebra mussel *Dreissena* in muddy offshore sediments of western Lake Erie, Canada. *Water Air Soil Pollut.* **99**: 623–632.
- DAME, R. F. 1996. Ecology of marine bivalves. CRC.
- DRAKE, D. E., D. A. CACCHIONE, AND W. D. GRANT. 1992. Shear stress and bed roughness estimates for combined wave and current flows over a rippled bed. *J. Geophys. Res.* **97**(C2): 2319–2326.
- DRAPER, N. R., AND H. SMITH. 1981. Applied regression analysis. Wiley.
- FAHNENSTIEL, G. L., G. A. LANG, T. F. NALEPA, AND T. H. JOHNGEN. 1995. Effects of zebra mussel (*Dreissena polymorpha*)

- colonization on water quality parameters in Saginaw Bay, Lake Huron. *J. Great Lakes Res.* **21**: 435–448.
- FANSLAW, D. L., T. H. NALEPA, AND G. A. LANG. 1995. Filtration rates of the zebra mussel (*Dreissena polymorpha*) on natural seston from Saginaw Bay, Lake Huron. *J. Great Lakes Res.* **21**: 489–500.
- FISCHER, H. B., E. J. LIST, R. C. Y. KOH, J. IMBERGER, AND N. H. BROOKS. 1979. Mixing in inland and coastal waters. Academic.
- FISHER, S. W., D. C. GOSSIAUX, K. A. BRUNER, AND P. F. LANDRUM. 1993. Investigations of the toxicokinetics of the hydrophobic contaminants in the zebra mussel (*Dreissena polymorpha*), p 465–490. *In* T. F. Nalepa and D. W. Schloesser [eds.], *Zebra mussels: Biology, impact, and control*. Lewis.
- FRÉCHETTE, M., C. A. BUTMAN, AND W. G. GEYER. 1989. The importance of boundary-layer flows in supplying phytoplankton to the benthic suspension feeder, *Mytilus edulis* L. *Limnol. Oceanogr.* **34**: 19–36.
- , D. LEFAIVRE, AND C. A. BUTMAN. 1993. Bivalve feeding and the benthic boundary layer, p. 325–369. *In* R. F. Dame [ed.], *Bivalve filter feeders*. Springer Verlag.
- FRETWELL, S. C. 1987. Food chain dynamics: the central theory of ecology? *Oikos* **50**: 291–301.
- GROSS, T. F., AND A. R. M. NOWELL. 1983. Mean flow and turbulence scaling in a tidal boundary layer. *Cont. Shelf Res.* **2**: 109–126.
- HAMBLIN, P. F. 1987. Meteorological forcing and water level fluctuations on Lake Erie. *J. Great Lakes Res.* **13**: 436–453.
- HEBERT, P. D. N., C. C. WILSON, M. H. MURDOCH, AND R. LAZAR. 1991. Demography and ecological impacts of the invading mollusc *Dreissena polymorpha*. *Can. J. Zool.* **69**: 405–409.
- HOLLAND, R. E., T. H. JOHNGEN, AND A. M. BEETON. 1995. Trends in nutrient concentrations in Hatchery Bay, western Lake Erie, before and after *Dreissena polymorpha*. *Can. J. Fish. Aquat. Sci.* **52**: 1202–1209.
- KOSEFF, J. R., J. K. HOLEN, S. G. MONISMITH, AND J. E. CLOERN. 1993. Coupled effects of vertical mixing and benthic grazing on phytoplankton populations in shallow estuaries. *J. Mar. Res.* **51**: 843–868.
- KRYGER, J., AND H. U. RIISGARD. 1988. Filtration rate capacities of European freshwater bivalves. *Oecologia* **7**: 34–38.
- KUNDU, P. K. 1990. *Fluid mechanics*. Academic.
- LEI, J., B. S. PAYNE, AND S. Y. WANG. 1996. Filtration dynamics of the zebra mussel, *Dreissena polymorpha*. *Can. J. Fish. Aquat. Sci.* **53**: 29–37.
- LUCAS, L. V., J. E. CLOERN, J. R. KOSEFF, S. G. MONISMITH, AND J. K. THOMPSON. 1998. Does the Sverdrup critical depth model explain bloom dynamics in estuaries? *J. Mar. Res.* **56**: 375–415.
- MACISAAC, H. J., W. G. SPRULES, O. E. JOHANSSON, AND J. H. LEACH. 1992. Filtering impacts of larval and adult zebra mussels (*Dreissena polymorpha*) in western Lake Erie. *Oecologia* **92**: 30–39.
- , O. E. JOHANSSON, J. YE, W. G. SPRULES, J. H. LEACH, J. A. MCCORQUODALE, AND I. A. GRIGOROVICH. 1999. Filtering impacts of an introduced bivalve (*Dreissena polymorpha*) in a shallow lake: Application of a hydrodynamic model. *Ecosystems* **2**: 338–350.
- MAKAREWICZ, J. C. 1993. Phytoplankton biomass and species composition in Lake Erie, 1970 to 1987. *J. Great Lakes Res.* **19**: 258–274.
- , T. W. LEWIS, AND P. BERTRAM. 1999. Phytoplankton composition and biomass in the offshore waters of Lake Erie: Pre- and post-*Dreissena* introduction (1983–1993). *J. Great Lakes Res.* **25**: 135–148.
- , P. BERTRAM, AND T. W. LEWIS. 2000. Chemistry of the offshore waters of Lake Erie: Pre- and post-*Dreissena* introduction (1983–1993). *J. Great Lakes Res.* **26**: 82–93.
- MONISMITH, S. G., J. R. KOSEFF, J. K. THOMPSON, C. A. O'RIORDAN, AND H. M. NEFF. 1990. A study of model bivalve siphonal currents. *Limnol. Oceanogr.* **35**: 680–696.
- MUNK, W., AND E. R. ANDERSON. 1948. Notes on a theory of the thermocline. *J. Mar. Res.* **7**: 276–295.
- NALEPA, T. F., AND D. W. SCHLOESSER. 1993. Zebra mussels: Biology, impact, and control. Lewis.
- NICHOLLS, K. H., G. J. HOPKINS, AND S. J. STANDKE. 1999. Reduced chlorophyll to phosphorus ratios in nearshore Great Lakes water coincide with the establishment of dreissenid mussels. *Can. J. Fish. Aquat. Sci.* **56**: 153–161.
- O'RIORDAN, C. A., S. G. MONISMITH, AND J. R. KOSEFF. 1995. The effect of bivalve excurrent jet dynamics on mass transfer in the benthic boundary layer. *Limnol. Oceanogr.* **40**: 330–344.
- RAUPACH, M. R., R. A. ANTONIA, AND S. RAJAGOPALAN. 1991. Rough-wall turbulent boundary layers. *Appl. Mech. Rev.* **13**: 97–129.
- REEDERS, H. H., AND A. BIJ DE VAATE. 1990. Zebra mussels (*Dreissena polymorpha*): A new perspective for water quality management. *Hydrobiologia* **200/201**: 437–450.
- , ———, AND F. J. SLIM. 1989. The infiltration of *Dreissena polymorpha* (Bivalvia) in three Dutch lakes with reference to biological water quality management. *Freshw. Biol.* **22**: 133–141.
- ROHLF, F. J., AND R. R. SOKAL. 1995. *Statistical tables*, 3rd ed. Freeman.
- SCHELSKE, C. L., AND D. A. HODELL. 1995. Using carbon isotopes of bulk sedimentary organic matter to reconstruct the history of nutrient loading and eutrophication in Lake Erie. *Limnol. Oceanogr.* **40**: 918–929.
- SPRUNG, M., AND U. ROSE. 1988. Influence of food size and food quality on the feeding of the mussel *Dreissena polymorpha*. *Oecologia* **77**: 526–532.
- TURNER, J. S. 1973. *Buoyancy effects in fluids*. Cambridge Univ. Press.
- [USEPA] U.S. ENVIRONMENTAL PROTECTION AGENCY. 1992. Methods for the determination of chemical substances in marine and estuarine samples. EPA/600/R-92/121. Environmental Protection Agency.
- WILDISH, D. J., AND D. D. KRISTMANSON. 1997. *Benthic suspension feeders and flow*. Cambridge Univ. Press.
- WU, L., AND D. A. CULVER. 1991. Zooplankton grazing and phytoplankton abundance: An assessment before and after invasion of *Dreissena polymorpha*. *J. Great Lakes Res.* **17**: 425–436.
- YAMAMURO, M., AND I. KOIKE. 1994. Diel changes of nitrogen species in surface and overlying water of an estuarine lake in summer: Evidence for benthic–pelagic coupling. *Limnol. Oceanogr.* **39**: 1726–1733.
- YU, N., AND D. A. CULVER. 1999. Estimating the effective clearance rate and refiltration by zebra mussels, *Dreissena polymorpha*, in a stratified reservoir. *Freshw. Biol.* **41**: 481–492.

Received: 8 March 2000

Accepted: 19 December 2000

Amended: 24 January 2001